The rates of Cu(ii)-ATCUN complex formation. Why so slow?

Kotuniak, Radosław; Szczerba, Paulina; Sudzik, Dobromiła; Strampraad, Marc J.F.; Hagedoorn, Peter Leon; Bal, Wojciech

DOI
10.1039/d2dt02856e

Publication date
2022

Document Version
Final published version

Published in
Dalton Transactions

Citation (APA)
Kotuniak, R., Szczerba, P., Sudzik, D., Strampraad, M. J. F., Hagedoorn, P. L., & Bal, W. (2022). The rates of Cu(ii)-ATCUN complex formation. Why so slow? *Dalton Transactions*, *51*(46), 17553-17557. https://doi.org/10.1039/d2dt02856e

Dalton Transactions

ROYAL SOCIETY OF CHEMISTRY

COMMUNICATION

View Article Online
View Journal | View Issue

Cite this: *Dalton Trans.*, 2022, **51**, 17553

Received 31st August 2022,
Accepted 14th November 2022

DOI: 10.1039/d2dt02856e

rsc.li/dalton

The rates of Cu(II)–ATCUN complex formation. Why so slow?†

Radosław Kotuniak,[a] Paulina Szczerba,[a] Dobromiła Sudzik,[a] Marc J. F. Strampraad,[b] Peter-Leon Hagedoorn [b] and Wojciech Bal *[a]

We used a series of modified/substituted GGH analogues to investigate the kinetics of Cu(II) binding to ACTUN peptides. Rules for rate modulation by 1st and 2nd sphere interactions were established, providing crucial insight into elucidation of the reaction mechanism and its contribution to biological copper transport.

Cu(II)–peptide interactions are crucially important for the understanding of copper speciation and transfer in body fluids and copper acquisition by cells. These issues have gained importance in the light of recent reports on copper imbalance in many diseases of civilization. A knowledge of reaction rates can help clarify such issues in copper physiology, as its cellular uptake or contribution to Alzheimer's disease pathology.[1] In biological processes the Cu(II) ions ought to be exchanged between different protein partners within strict timeframes. For instance, the hCTR1 cellular transporter apparently requires just 100 ms to deliver a copper ion to a cell,[2] while Cu(II) release and reuptake in the synaptic cleft occur within a few milliseconds.[3] Studies on the kinetics of Cu(II)–peptide complex formation have rarely been undertaken over the past two decades, even though technical possibilities to perform such experiments are available, and valuable results have been obtained occasionally.[4] Rapid mixing techniques can strongly complement the classical steady-state approach in an effort to elucidate studied processes.

The proteins and peptides possessing the ATCUN (amino-terminal copper and nickel) motif are considered to be physiological Cu(II) carriers.[5,6] The ATCUN sequence consists of the His3 residue preceded by any two amino acid residues, except Pro2, and possesses a free amine group at the N-terminus. In the physiological pH range its Cu(II) complex is square planar, with a four-nitrogen (4N) coordination mode (Fig. 1). ATCUN complexes found in human proteins, *e.g.* albumin (N-terminal sequence DAH),[7] copper importer hCtr-1 (MDH)[8] or $A\beta_{4-x}$ peptides (FRH),[9] exhibit pico- to femtomolar Cu^{2+} affinities at pH 7.4.[1,5] However, despite the vast knowledge about Cu(II) complexes with these and other ATCUN sequences, obtained from potentiometric, spectroscopic (UV-Vis, CD), structural (X-ray, NMR, EXAFS) or electrochemical studies, little is known about the mechanisms and rates of their formation.

Previously, we studied the formation of the GGH–Cu(II) complex, the simplest ATCUN representative using stopped-flow with diode-array detection, microsecond freeze hyperquenching (MHQ) and electrochemistry.[10] Overall, the binding reaction took almost one second, according to the following scheme. First, within about 100 μs after mixing Cu^{2+} and GGH solutions, an "early complex" (EC) was formed with Cu^{2+} bound to the peptide *via* a single nitrogen atom (1N coordination). The attachment of the second nitrogen atom (2N) was completed within 2 ms after mixing. This "intermediate complex" (IC) exhibits a UV-Vis band with $\lambda_{max} \approx 700$ nm and includes the Cu(II) bound at the imidazole and N-terminal amine nitrogen atoms (NH_2 + N_{Im}). Finally, IC converts ($t_{1/2} \approx$ 100 ms) into the stable 4N (λ_{max} = 525 nm). However, the resolution of the available spectroscopic techniques was not

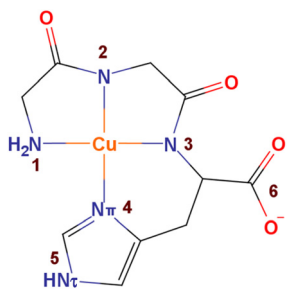

Fig. 1 The structure of the GGH–Cu complex at neutral pH (4N). Modified atoms are numbered for clarification.

[a]*Institute of Biochemistry and Biophysics, Polish Academy of Sciences, Pawińskiego 5a, 02-106 Warszawa, Poland. E-mail: wbal@ibb.waw.pl*
[b]*Department of Biotechnology, Delft University of Technology, Van der Maasweg 9, 2629 HZ Delft, The Netherlands*

†Electronic supplementary information (ESI) available: Materials and methods, supplementary figures with experimental data and structures of studied peptides/complexes, additional references. See DOI: https://doi.org/10.1039/d2dt02856e

sufficient to elucidate the exact coordination geometries of the EC and IC complexes. For the latter we proposed a *cis–trans* isomerisation as a source of its long lifetime (see Fig. S1† for the reaction mechanism proposed in ref. 10), but other possibilities should also be considered, such as the contribution of the C-terminal carboxylate. GGH does not have side chains, but all biological ATCUN peptides do. Their influence on the reaction rate remains unknown, and needs to be investigated.

To approach the first of these issues we synthesized five GGH analogues, each having one nitrogen atom blocked from Cu(II) coordination (see Fig. 1 and Fig. S2†). The N-terminal amine nitrogen was blocked by acetylation (Ac), while other positions were blocked by methylation (Me). The modifications of amide nitrogens, marked as 2 and 3 in Fig. 1, yielded G(N–Me)GH and GG(N–Me)H, respectively. Substitutions of the imidazole ring nitrogens, numbered 4 and 5 in Fig. 1, yielded GG(Nτ–Me)H and GG(Nπ–Me)H. The sixth derivative was C-terminally amidated, to mimic longer peptides (GGH-am). The Cu^{2+} binding to each peptide was examined by the stopped-flow diode-array system. Respective 4 mM solutions of these peptides in 400 mM MES buffer, pH 6, were reacted with mildly acidic (pH 4) aqueous solutions of $CuCl_2$. The reactions were followed by recording full UV-Vis spectra every 9.9 or 0.66 ms using a diode array detector. These experimental conditions were chosen to avoid interference from the buffer and to avoid $Cu(OH)_2$ precipitation.[10] Additionally, pH-metric titrations with UV-Vis and CD detection were performed for each studied system.

The C-terminal amidation of GGH did not alter the final 4N complex structure (structure **6** in Fig. S2†) as confirmed by UV-Vis and CD pH-metric titration results (Fig. S3 and S8A†), compared to GGH,[11] but its formation took almost four times longer (Fig. 2).[10] A species with an initial band at around 715 nm was not visible in the steady-state data, but based on the GGH study it can be assigned to the IC/2N complex.[10] These differences indicate the paradoxical involvement of the COO^- group, enhancing the formation of the 4N complex. Recent DFT calculations indicate a possible axial binding of the carboxyl oxygen in a 2N type species.[12] This may affect the *cis*/*trans* equilibrium enhancing the relative abundance of the effective *cis–exo* isomer, which precedes the 4N complex in the mechanism proposed previously (Fig. S1†).[10] Targeted theoretical calculations are needed to clarify this issue.

The kinetic traces for Cu^{2+} binding to GG(Nτ–Me)H and GG(Nπ–Me)H are presented in Fig. 3, in comparison to GGH. Full kinetic spectra are presented in Fig. S8C and D,† while Fig. S4A and B† provide the corresponding steady-state spectroscopic titrations. Unlike GGH, the mixing of GG(Nπ–Me)H with Cu^{2+} ions produced a relatively slow, homogeneous increase of a band at 625 nm. Blocking Nπ disabled the formation of the 5,5,6-chelate of the 4N ATCUN complex (Fig. 1). The alternative 5,5,7-system *via* Nτ is entropically disfavoured. Instead, as confirmed by pH-metric titrations, a different complex, formed with pK = 5.44, provided the reaction endpoint at pH 6 (see Fig. S4A†). Its absorption maximum at 625 nm and the positive CD band at around 615 nm indicate the formation of a 3N form with $\{NH_2 + N^- + N_{Im}\}$ coordi-

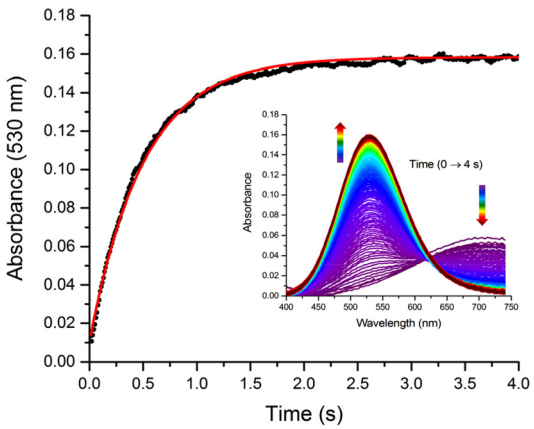

Fig. 2 Kinetic curve for the reaction of 2 mM GGH-am with 1.6 mM Cu(II) at pH = 6.0 in 200 mM MES generated for the maximum reaction product absorption. The inset shows whole spectra for the same experiment, recorded every 9.9 ms with a diode-array stopped-flow system.

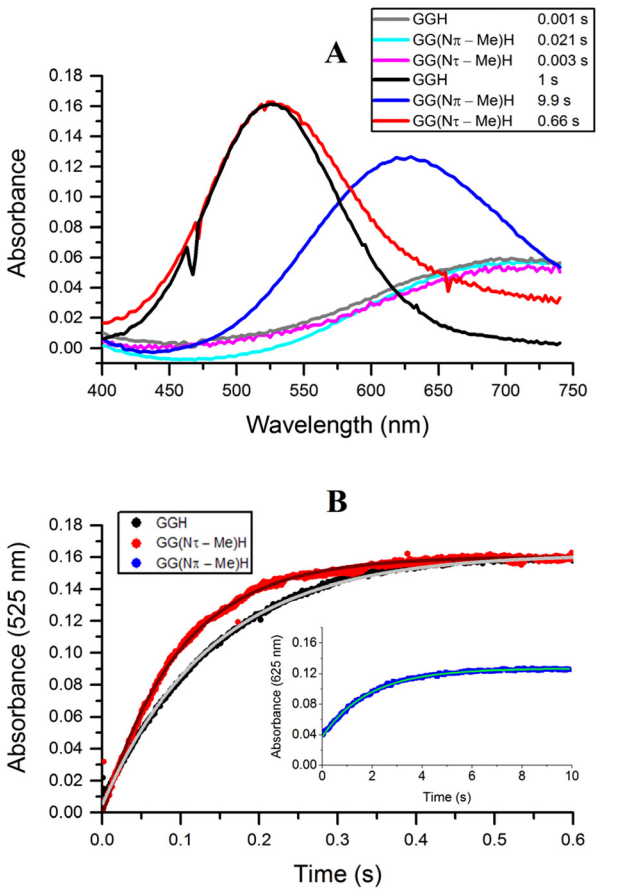

Fig. 3 Diode-array stopped-flow experiment for 1.6 mM Cu(II) reacted with 2 mM GG(π-Me)H or GG(τ-Me)H in comparison to the reaction with GGH from ref. 10. Plot (A) shows the kinetic spectra at the beginning and the end of each reaction. Plot (B) shows the kinetic curves at the maximum absorbance of the final complex.

nation (structure **4** in Fig. S2†). This involves the glycyl peptide nitrogen being stabilized by the 5-membered ring with the N-terminal amine and Nτ, as there would be no CD signal if Cu(II) were coordinated to Gly donors only. The formation of the single 5-membered chelate ring in GG(Nπ–Me)H is unexpectedly much slower ($t_{1/2}$ = 1.29 s) than in GGH ($t_{1/2}$ = 0.096 s).[10] At a higher pH this species (with an isosbestic point at 610 nm in UV-Vis spectra) is directly replaced by a complex with a d–d maximum at 545 nm, and a stronger negative N^-–Cu(II) CD band at around 300 nm (pK = 8.64, Hill coefficient n = 1.28). Judging from a red-shift of this band relative to the one in ATCUN and the absence of a split CD d–d pattern, we assign this species as an $\{NH_2 + N^- + N^-\}$ chelate complemented with an OH^- derived from a water molecule.

The reaction of GG(Nτ–Me)H was qualitatively very similar to that of GGH, yielding the 4N complex (structure **5** in Fig. S2†) as the end product (Fig. 3A and S4C, D†) with $t_{1/2}$ = 67 ms, slightly faster than that for GGH, $t_{1/2}$ = 96 ms (Fig. 3B). The spectra recorded at the beginning of reactions (Fig. 3A) for these three peptides are barely distinguishable. This means that the IC, and presumably the EC, in GGH can involve either Nτ or Nπ. The faster 4N formation for GG(Nτ–Me)H is due to the elimination of the reaction pathway *via* Nτ, which is unproductive in terms of the 4N complex formation (Fig. S1†). Assuming that the 4N complex formation rate in GGH *vs.* GG(Nτ–Me)H would be proportional to the relative Cu(II) occupancy of Nπ (productive) *vs.* Nτ (unproductive) in the GGH IC, and considering the default Nπ occupancy in GG(Nτ–Me)H, one obtains the Nπ occupancy in the GGH IC as 67/96 = 0.7. This value is in perfect agreement with the tautomeric imidazole protonation pattern in *N*-Ac-His-methylamide, that is 0.71.[13]

The amine nitrogen acetylation shifted the formation of Cu(II) chelate rings to an alkaline pH (Fig. S5 and S6†). Judging from the d–d band position at around 750 nm, the imidazole-bound EC (structure **1** in Fig. S1†) is thermodynamically stable at pH 6. As expected, it was formed within the stopped-flow dead time and remained unchanged during the measurement (Fig. S5 and S8B†).

The two remaining peptides in this series had individually methylated peptide bond nitrogens. The pH titration of the Cu(II)GG(N–Me)H complex presented in Fig. S7† revealed a 3N complex as the final species at pH 6 and above (pK = 5.16; n = 1.7). Accordingly, the kinetic experiment traced its formation from IC (Fig. S5 and S8E†) along the spectral shift from 695 nm to 625 nm. The product was very similar to Gly–Gly–(Nπ–Me)His (structure **3** in Fig. S2†), but the reaction was faster ($t_{1/2}$ of 478 ms *vs.* 1294 ms). The ratio of respective rates apparently reflects the higher thermodynamic stability of CuGG(N–Me)H (*viz.* pK 5.16 *vs.* 5.44), mediated by a more favourable conformation of the peptide having the Nπ available for Cu(II) binding.

The Cu(II) complex with G(N–Me)GH can assume the 3N coordination only through the formation of a six-membered ring with the His peptide nitrogen. This is a less stable arrangement; hence it is formed above pH 6. At pH 6 the spectroscopic titrations indicated an IC type complex (structure **2** in Fig. S2†). This is fully confirmed by the stopped-flow study, where the IC formed within the reaction dead time remained unchanged throughout the observation time (Fig. S5 and S8F†).

With the obvious exception of Ac-GGH, the IC complex with the $\{NH_2 + N_{Im}\}$ coordination mode was the earliest species uniformly seen in stopped-flow experiments for GGH analogues (Fig. S5C†). The stopped-flow studies did not exhibit initial bands that could be ascribed to alternative $\{N_{Im} + N^-\}$ or $\{NH_2 + N^-\}$ species. This could be explained by the slowness of formation of the single Cu(II)–N^- bond, demonstrated in the 3N species formation for GG(Nπ–Me)H and GG(N–Me)H. It is intriguing that two adjacent Cu(II)–N^- bonds in GGH, GGH-am and GG(Nτ–Me)H were formed so much faster in otherwise very similar peptides. Furthermore, despite the nonequivalence of Gly and His amide nitrogens in terms of Cu(II) binding demonstrated above, we never observed 3N intermediates on the path to 4N species. These features, perhaps dictated by peptide chain conformations, warrant further experimental and computational studies.

For the second issue, we studied how specific side chains in regular ATCUN oligopeptides affected the rate of IC to 4N conversion. This is important, as natural ATCUN peptides and proteins usually possess non-glycine amino acids.[14] For this purpose we synthesized a set of model peptides (listed in Table 1) and determined their Cu^{2+} binding reaction rates. For all studied peptides the reaction proceeded as for GGH in terms of spectral parameters of the first detected (IC) and the final (4N) products. The λ_{max} values differed by less than 10 nm, except the IC for EGHG-am, which shifted by 20 nm from the average value (Fig. S9†). The direct IC to 4N conversion was evident from isosbestic points at 615 nm (Fig. S10 and S11†). Two peptides (GGHG-am and GGHGGG-am) were used to investigate the role of peptide chain elongation. As presented in Table 1, it had no effect on the rate, compared to GGH-am. This allowed us to use GGHG-am as a template for single substitutions of Gly residues. We chose three substitutions: hydrophobic Leu, negatively charged Glu and posi-

Table 1 Reaction half times ($t_{1/2}$) for Cu(II) binding with modified peptides. Acceleration factors (AFs) were calculated with respect to the reaction Cu(II) + GGH-am.

Position	Sequence	$t_{1/2}$ (s)	AF
	GGH	0.0969 ± 0.0002	3.61
C-terminus	GGH-am	0.3499 ± 0.0016	1.00
	GGHG-am	0.3447 ± 0.0015	1.02
	GGHGGG-am	0.3563 ± 0.0017	0.98
First	LGHG-am	0.2871 ± 0.0012	1.22
	KGHG-am	0.2103 ± 0.0007	1.66
	EGHG-am	1.6915 ± 0.0088	0.21
Second	GLHG-am	1.9262 ± 0.0026	0.18
	GKHG-am	0.8738 ± 0.0019	0.40
	GEHG-am	0.7406 ± 0.0026	0.47
Fourth	GGHL-am	0.2497 ± 0.0009	1.40
	GGHK-am	0.2487 ± 0.0010	1.41
	GGHE-am	0.1666 ± 0.0007	2.10

tively charged Lys. We considered these substitutions to have little effect on the first coordination sphere of the 4N complex, hence allowing us to focus on the properties of the IC and the reaction pathway. All amino acid residues are larger than glycine, which causes additional steric hindrance. To keep this effect consistent, we selected residues with side-chain volumes possibly similar to each other (Leu 178.7 Å^3, Glu 140.2 Å^3, Lys 170.3 Å^3 *versus* Gly 71.7 Å^3).[15] The kinetic traces from stopped-flow diode-array experiments are shown in Fig. 4, while Table 1 presents the reaction half-times. The acceleration factor (AF) was calculated relative to the Cu^{2+} reaction with GGH-am.

The obtained results show intriguing correlations between the position of the substituted amino acid and the reaction rate. The presence of a non-glycine residue in the 4th position surprisingly accelerated the 4N complex formation. This effect was observed even though the previously mentioned peptide chain elongation with glycines did not affect the binding rate. In contrast, Gly substitution in the 2nd position inhibited the reaction in all studied cases. The situation in the 1st position appears to be more complicated, with Lys and Leu accelerating the reaction and Glu inhibiting it. One should, however, consider that the spectrum of the EGHG-am IC was blue-shifted from all others and had a clearly higher intensity (Fig. S9†). These features show that Glu1 carboxylate binds the Cu(II) ion in IC, enhancing its stability and thus diminishing its reactivity. With this exception, one can clearly notice that the side-chain volume rather than the charge controls the reaction rate. Our data show that the IC to 4N reaction is enhanced by the bulkiness near the Cu(II) binding nitrogens and slowed down by steric hindrance in the middle, near the peptide nitrogens. This finding is consistent with our previous proposal that the IC to 4N transition rate in GGH, and presumably other ATCUN peptides, is controlled by conformational equilibria in the IC.[1,10]

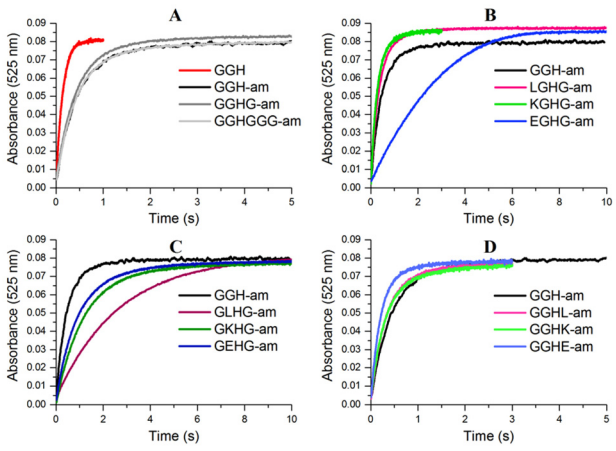

Fig. 4 Kinetic curves for the reaction of Cu(II) with (A) longer peptides, and with GGHG-am derivatives substituted at the first (B) second (C) or third (D) positions. Reference data for GGH and GGH-am were rescaled for the sake of comparison.

To conclude, in this study we systematically analysed the effect of the 1st and 2nd sphere on the rate of formation of cupric 4N ATCUN complexes, first reported for the GGH tripeptide.[10] Data for GGH analogues with respective nitrogen atoms excluded from Cu(II) binding revealed that despite the absence of a chelate effect, the formation of a metastable IC complex with $\{NH_2 + N_{Im}\}$ coordination is more than a hundred-fold faster than the $\{NH_2 + N^-\}$ or $\{N^- + N_{Im}\}$ alternatives. The series of Gly-substituted GGHG-am analogues revealed the relevance of steric hindrance in reaction rate modulation. This supports the original concept of reaction rate control by *cis–trans* coordination equilibria and peptide main-chain conformation (Fig. S1†). However, the reaction acceleration by His carboxylate in GGH and inhibition by the Glu1 carboxylate in EGHG-am, indicates that additional Cu(II) binding phenomena in the EC or the IC may exert crucial reaction control in specific cases. Main-chain elongation beyond the fourth residue did not affect the rate of 4N complex formation, but the individual non-Gly substitutions may. These systematic findings provide the basis for experimental studies on actual biological peptides and for molecular dynamics studies of the reaction mechanism.

Conflicts of interest

There are no conflicts to declare.

Acknowledgements

This research was financed by the National Science Centre of Poland (NCN) grant no. 2018/31/N/ST5/02556. The equipment used at IBB PAS was sponsored, in part, by the Centre for Preclinical Research and Technology (CePT), a project co-sponsored by the European Regional Development Fund and Innovative Economy, the National Cohesion Strategy of Poland.

References

1 R. Kotuniak and W. Bal, *Dalton Trans.*, 2022, **51**, 14–26.
2 E. B. Maryon, S. A. Molloy, K. Ivy, H. Yu and J. H. Kaplan, *J. Biol. Chem.*, 2013, **288**, 18035–18046.
3 W. Goch and W. Bal, *PLoS One*, 2017, **12**, e0170749.
4 (*a*) T. Branch, P. Girvan, M. Barahona and L. Ying, *Angew. Chem., Int. Ed.*, 2015, **54**, 1227–1230; (*b*) J. T. Pedersen, K. Teilum, N. H. H. Heegaard, J. Østergaard, H.-W. Adolph and L. Hemmingsen, *Angew. Chem.*, 2011, **123**, 2580–2583.
5 P. Gonzalez, K. Bossak, E. Stefaniak, C. Hureau, L. Raibaut, W. Bal and P. Faller, *Chem. – Eur. J.*, 2018, **24**, 8029–8041.
6 (*a*) M. D. J. Libardo, A. A. Bahar, B. Ma, R. Fu, L. E. McCormick, J. Zhao, S. A. McCallum, R. Nussinov, D. Ren, A. M. Angeles-Boza and M. L. Cotten, *FEBS J.*, 2017, **284**, 3662–3683; (*b*) T. T. K. Nguyen, H. V. Tran, T. T. Vu, S. Reisberg, V. Noël, G. Mattana, M. C. Pham and B. Piro, *Biosens. Bioelectron.*, 2019, **127**, 118–125;

(*c*) H. Moulahoum, F. Ghorbani Zamani, S. Timur and F. Zihnioglu, *Probiotics Antimicrob. Proteins*, 2020, **12**, 48–63.
7 (*a*) W. Bal, M. Sokołowska, E. Kurowska and P. Faller, *Biochim. Biophys. Acta, Gen. Subj.*, 2013, **1830**, 5444–5455; (*b*) T. Peters, *Adv. Protein Chem.*, 1985, **37**, 161–245.
8 (*a*) K. L. Haas, A. B. Putterman, D. R. White, D. J. Thiele and K. J. Franz, *J. Am. Chem. Soc.*, 2011, **133**, 4427–4437; (*b*) E. Stefaniak, D. Płonka, S. C. Drew, K. Bossak-Ahmad, K. L. Haas, M. J. Pushie, P. Faller, N. E. Wezynfeld and W. Bal, *Metallomics*, 2018, **10**, 1723–1727.
9 (*a*) M. Mital, N. E. Wezynfeld, T. Frączyk, M. Z. Wiloch, U. E. Wawrzyniak, A. Bonna, C. Tumpach, K. J. Barnham, C. L. Haigh, W. Bal and S. C. Drew, *Angew. Chem., Int. Ed.*, 2015, **54**, 10460–10464; (*b*) E. Stefaniak and W. Bal, *Inorg. Chem.*, 2019, **58**, 13561–13577.
10 R. Kotuniak, M. J. F. Strampraad, K. Bossak-Ahmad, U. E. Wawrzyniak, I. Ufnalska, P.-L. Hagedoorn and W. Bal, *Angew. Chem., Int. Ed.*, 2020, **59**, 11234–11239.
11 K. Bossak-Ahmad, T. Frączyk, W. Bal and S. C. Drew, *ChemBioChem*, 2020, **21**, 331–334.
12 J. Heinrich, K. Bossak-Ahmad, M. Riisom, H. H. Haeri, T. R. Steel, V. Hergl, A. Langhans, C. Schattschneider, J. Barrera, S. M. F. Jamieson, M. Stein, D. Hinderberger, C. G. Hartinger, W. Bal and N. Kulak, *Chem. – Eur. J.*, 2021, **27**, 18093–18102.
13 M. Tanokura, *Biochim. Biophys. Acta, Protein Struct. Mol. Enzymol.*, 1983, **742**, 576–585.
14 T. Frączyk, *Chem. Biodiversity*, 2021, **18**, e2100043.
15 A. E. Counterman and D. E. Clemmer, *J. Am. Chem. Soc.*, 1999, **121**, 4031–4039.